International Journal of Signal Processing, Image Processing and Pattern Recognition
Vol. 8, No. 4 (2015), pp. 181-190
http://dx.doi.org/10.14257/ijsip.2015.8.4.16

Change Detection Algorithm on Wavelet and Markov Random Field

Song Hongxun, Wang Weixing, Zhang Tingting, Yu Tianchao and Song Junfang

Shaanxi Road Traffic Intelligent Detection and Equipment Engineering Technology Research Center, Chang'an University, Xi'an, China
School of Information Engineering, Chang'an University, Xi'an, China
songhongx @163.com

Abstract

In this study, the algorithm that applies Wavelet and multi-scale analysis to remote sensing images is proposed for region variation detection on Markov random field. First of all, the Wavelet transform is adopted to decompose an original image into several sub-images, then the Mahalanobis distance decision function is used to detect the changes in different scale images, and finally the Markov random field is applied to fuse the change detection results at different scales. Since the Markov random field fusion method takes full account of the correlation between the adjacent pixels and the links of the change detection results at different scales, the fusion results are accurate and practical. The testing results prove that the studied algorithm is effective and robust.

Keywords: *Change Detection, Multi-Scale, Mahalanobis distance, Markov Random Field, Image Fusion*

1. Introduction

A change (change) detection method/algorithm is used for detecting the change information of the surface features in an area, by analyzing the differences between remote sensing images of the same area at different times [1-2]. As the aerospace, remote sensing and information technology development, the change detection has been widely applied for monitoring urban land change, forest vegetation cover change, for evaluating natural disasters such as earthquake, floods, forests fires, as well as for estimating military strike effort [1-3].

In general, a traditional change detection algorithm includes three work steps [4]: image pre-processing, change detection and image post-processing. The image pre-processing algorithms in different change detection algorithms are slightly different, but the image registration is an important and indispensable step [5]. Image registration accuracy obviously affects change detection results, so Dai and Siamak (1998) [6] studied in depth how image registration accuracy impact to change detection, pointing out that image registration error needed to be less than one pixel to meet the requirement of change detection. Normally, the image registration accuracy is difficult to meet application requirements, in such cases, the image post-processing is demanded to remove the fake changes caused by the registration error and noise through different image filters. Although this is a human-computer interaction process, the outcome cannot be satisfactory. In order to overcome the effects of the image registration, some researchers have already put forward various algorithms, such as (1) object-based algorithm [7-9], (2) match-based algorithm [10], namely the approach of the image registration and the change detection at the same time. The object-based approach [9] is mainly dependent on the accuracy of the target detection, and the match-based approach is more complicated and difficult than the others.

ISSN: 2005-4254 IJSIP
Copyright ⓒ 2015 SERSC

The multi-scale analysis technique is widely used in the digital image processing and analysis. The change detection results between the different scale remote sensing images over the same area at different times are different [11], so some researchers have applied the multi-scale analysis into the change detection at different angles, such as Huo, *et al.*, (2008) [7] proposed an object-based multi-scale change detection algorithm, and Francesca and Lorenzo (2005) [12] studied a multi-driven- based change detection algorithm. The algorithm studied in this paper is based on but different to the above two algorithms. It is a new wavelet and multi-scale analysis algorithm applied to the change detection. The main idea is to fuse the change detection results at different scales by using the Markov random field. It belongs to the pixel level fusion, but it takes the full account of the correlation between the adjacent pixels and the links of change detection results at different scales, so the obtained change regions are more coherent, the wrong detection results caused by the registration error and noise are more effectively to overcome. And the algorithm is a fully automatic process method, and the main principles and flowchart are shown in Figure 1.

The paper is organized as: Section 2 briefly describes the basic principle of the wavelet-based multi-scale decomposition; Section 3 expatiates change detection based on the Mahalanobis distance and its fast processing function; Section 4 is about the Markov random field theory applied into the fusion of the change detection results at different scales; the experimental data and result analyses are given in Section 5; and finally, Section 6 is the conclusion.

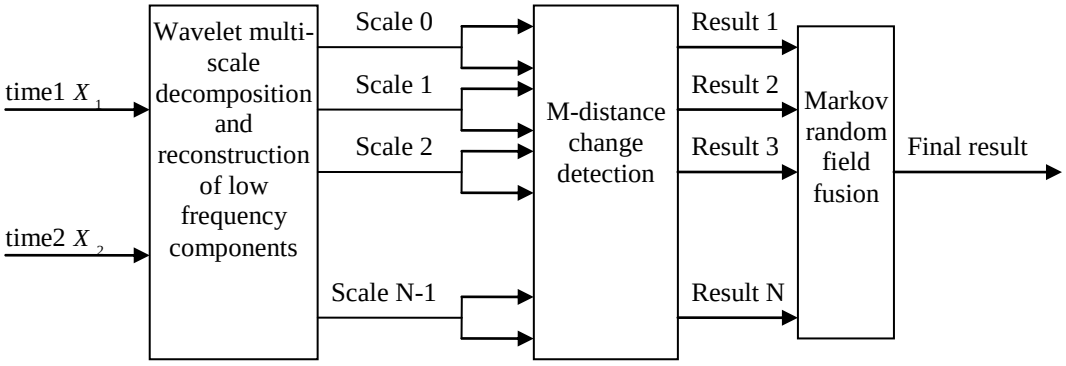

Figure 1. Change Detection based on Multi-scale Fusion Principles

2. Image Decomposition based on Wavelet Transform

The study uses the wavelet transform to carry out the multi-scale decomposition of the two remote sensing images at different times for the multi-scale fusion [12-14]. The two remote sensing images $X_k(k=1,2)$ at different times through the wavelet transform can be decomposed into the two multi-scale remote sensing image sequences $X_{MS}^{k}=\{X_{MS}^{(k,0)}\ldots X_{MS}^{(k,n)}\ldots X_{MS}^{(k,N-1)}\}(k=1,2)$, where, the number N is for the decomposition layer, and the images $X_{MS}^{(k,0)}=X_k$ are the original scale images. Each scale image $X_{MS}^{(k,n)}$ consists of four parts $X_{MS}^{(k,n)}=\{LL^{(k,n)},LH^{(k,n)},HL^{(k,n)},HH^{(k,n)}\}$, where, the images $LL^{(k,n)}$ stand for the low frequency information images, and the images $LH^{(k,n)},HL^{(k,n)},HH^{(k,n)}$ respectively stand for the high frequency information images in the horizontal, vertical, and diagonal directions. For the different scale

 Copyright ⓒ 2015 SERSC

number n , the images $X_{MS}^{(k,n)}$ reflect both the low frequency and high frequency information of the different scale images. In order to fuse the results at different scales, the algorithm reconstructs the low frequency information $LL^{(k,n)}$ at each scale, and makes the scale sizes as the same as those in the original images. The multi-scale reconstructed image sequences $X_{MS}^{k} = \{LL^{(k,0)} \ldots LL^{(k,n)} \ldots LL^{(k,N)}\} (k = 1, 2)$ are rebuilt, where, the reconstructed images in the same scale with the low frequency and at different times can be used for the change detection through the Mahalanobis distance change detection method. In this way, the obtained results at different scales are fused through the Markov random field to form a more accurate and practical result.

3. Change Detection on Mahalanobis Distance

In a change detection algorithm, the image differencing is usually used to describe the changes between two images. Hence, the multidimensional differenced images between two changed images can be used to construct a feature space for describing the changes. In a multidimensional Gaussian feature space, a hyper-ellipsoidal decision surface between change and non-change is more representative than any other kind of decision surfaces. And the change signal can be approximately modeled by a Gaussian distribution, so the Mahalanobis distance function for an n-dimensional difference image can be utilized as a decision function between change and non-change [6]. It can be described as:

$$M_d(i, j) = \sqrt{(X(i, j) - u)^T \Sigma^{-1} (X(i, j) - u)} \tag{1}$$

Where, the image $X = | X_1 - X_2 |$ stands for the multi-spectral differenced image, the value $X(i, j)$ are for the pixel values of the differenced images, and the symbols μ and Σ are for the total mean vector and covariance matrix respectively. One can also use the other Mahalanobis distance expression as:

$$M_d(i, j) = \sqrt{(X_1(i, j) - X_2(i, j))^T \Sigma^{-1} (X_1(i, j) - X_2(i, j))} \tag{2}$$

Where, the symbol Σ is for a mutual covariance matrix. The direct calculation of equations (1) and (2) is more complicated and slower, which can be improved through the following operations. The covariance matrix Σ can be orthogonal decomposed as:

$$\Sigma^{-1} = E \Lambda E^T \tag{3}$$

Where, the symbol E is composed of orthogonal transformation matrix that consists of the eigenvectors of the covariance matrix Σ . The symbol Λ is a characteristic matrix.

$$\Lambda = \begin{bmatrix} \lambda_1 & \cdots & 0 \\ \cdots & \cdots & \cdots \\ 0 & \cdots & \lambda_N \end{bmatrix} \tag{4}$$

Where, N is the band number. Suppose that

$$X'(i, j) = E^T * (X(i, j) - \mu) \text{ or } X'(i, j) = E^T * (X_1(i, j) - X_2(i, j)) \tag{5}$$

One can get

$$M_d(i, j) = \sqrt{X'(i, j)^T \Lambda X'(i, j)} \tag{6}$$

Copyright ⓒ 2015 SERSC

Let $X'(i, j) = (x_1', x_2', ..., x_N')$ is as a vector, and then

$$M_d(i, j) = \sqrt{\frac{x_1'^2}{\lambda_1} + \frac{x_2'^2}{\lambda_2} + \cdots + \frac{x_N'^2}{\lambda_N}} \tag{7}$$

Further, the change detection based on the Mahalanobis distance can be described as follows:

$$\begin{cases} M_d(i, j) < threshold & unchanged \\ M_d(i, j) \geq threshold & changed \end{cases} \tag{8}$$

Where, the threshold value can be set experience and image resolution.

4. Markov Random Field Fusion

Generally, the changed pixel decision result based on a threshold is usually affected by image registration errors, so the change result image has a large number of noise points. Because the link between the adjacent pixels is not considered, and the obtained change regions are often not continuous. In this study, the Markov random field [15-16] is applied and the correlation between the adjacent pixels and the links of the change detection results at different scales are taken full account, in this way, the fusion results are more accurate and practical.

The image X of the size $I \times J$ can be considered as a random field. In the image X, each pixel range is limited at $x \in \Lambda = \{0,1,..., L-1\}$, such as the gray image $L = 256$ and the obtained result image $\Lambda = \{0,1\}$. The collection $C = \{C_l, 1 \leq l \leq 2^{I*J}\}$ constructs all the possible result images. The multi-scale change detection result images $A = \{A_1, A_2, ...A_N\}$ are used to obtain the final change result image, which belongs to maximizing a posteriori probability problem [17]. It can be described as:

$$P(Y^* / A) = \max_{Y \in C}\{P(Y / A)\} \tag{9}$$

When the multi-scale change detection result image A is known, it is equal to equation:

$$P(Y^*, A) = \max_{Y \in C}\{P(Y, A)\} \tag{10}$$

As shown in equation (10), it is a global optimization problem and is difficult to solve, so the Markov random field is utilized to transform it to a local optimization problem. In this study, the second-order neighborhood $S = \{(i \pm 1, j), (i, j \pm 1), (i \pm 1, j \pm 1)\}$ for each pixel (i, j) is chosen, and the frame (Y, S) is considered as a Markov random field. And the Markov random field is equal to Gibbs random field [18]:

$$P(Y, A) = Z^{-1} \exp[-U(Y, A)] \tag{11}$$

Where, Z is a normalization constant and $U(Y, A)$ is a Gibbs power function. The maximum posteriori probability problem is transformed into a minimum power function problem in the Gibbs random field. The power function for each pixel (i, j) can be expressed by using its second-order neighborhood power function:

$$U(Y_{ij}, Y, A) = U(Y_{ij}, Y_{mn}, A_{mn}, (m, n) \in S) \tag{12}$$

The total power function is

 Copyright ⓒ 2015 SERSC

$$U(Y, A) = \sum_{i=1}^{I} \sum_{j=1}^{J} U(Y_{ij}, Y, A) \tag{13}$$

One can minimize each pixel (i, j) power function $U(Y_{ij}, Y, A)$ to make the total power function $U(Y, A)$ be a minimum. ICM (Iterated Conditional Modes (ICM) algorithm [19]. can be available to solve this. And the power function $U(Y_{ij}, Y, A)$ is divided into two parts: the first part $U_1(Y_{ij}, Y_{mn}, (m, n) \in S)$ stands for the correlation between the adjacent pixels, and the second part $U_2(Y_{ij}, A_{mn}, (m, n) \in S)$ for the connection between the pixels in each scale result and in the final result A. The two part power functions are respectively defined as:

$$U_1(Y_{ij}, Y_{mn}, (m, n) \in S) = -\alpha \sum_{(m,n) \in S} I(Y_{ij}, Y_{mn}) \tag{14}$$

$$U_2(Y_{ij}, A_{mn}, (m, n) \in S) = -\sum_{k=1}^{N} \beta_k \sum_{(m,n) \in S} I(Y_{ij}, A_{mn}^k) \tag{15}$$

$$I(y_1, y_2) = \begin{cases} 1, & y_1 = y_2 \\ 0, & y_1 \neq y_2 \end{cases} \tag{16}$$

Where, $\alpha, \beta_k (1 \leq k \leq N)$ are cycle weight coefficients to control the convergence condition. The overall algorithm steps are as follows:

(1) Firstly decompose two remote sensing images at different times through the 2-D wavelet transform, and then reconstruct low frequency components to make their sizes as the same as those in the original images. Finally obtain the two sets of the multi-scale image sequences
(2) In two sets of the multi-scale images sequences, detect the same scale image change through the Mahalanobis distance and get the final result through a threshold segmentation algorithm.
(3) Set equation $\alpha = 0$, initialize Y by minimizing the second part power function $U_2(Y_{ij}, A_{mn}, (m, n) \in S)$.
(4) Set $\alpha = 1$, refresh Y to make the total power function minimum, at the same time the cycle end condition is decided. When the change number of Y at the two times is less than a certain value, it ends.
(5) Decide if cycle times are over, if not, go back to (4).

5. Test Results and Analysis

A number of sets of data are used for testing; all the testing results prove that the studied algorithm is effective. As an example, one of the test data is from the following net: http://shr.aaas.org/geotech/gaza/gaza.shtml, and it is illustrated in Figures 2(a-b).

In Figure 2, the image (a) and the image (b) are the two remote sensing images taken by IKONOS satellite in the same place at different times, and the image resolution is of 980×612 pixels. From the images, one can see the changes between them. As shown in Figure 2, after 5 months, the area was destroyed by a disaster, and the blue houses and some green lands were disappeared. The image (c) is the reference change result, the image (d) is the processing result by the algorithm in this study, the image (e) is the result obtained by the Mahalanobis distance change

Copyright ⓒ 2015 SERSC

detection and post-processing, the image (f) is the result by using the reference method (Huo, *et al.*, 2008), and the images (g), (h) and (i) are the change detection results at three different scales. Table 1 is obtained through stating detection rate, accuracy and kappa coefficient to compare the properties of the results by using different algorithms and the results are taken at different scales (0, 1, 2).

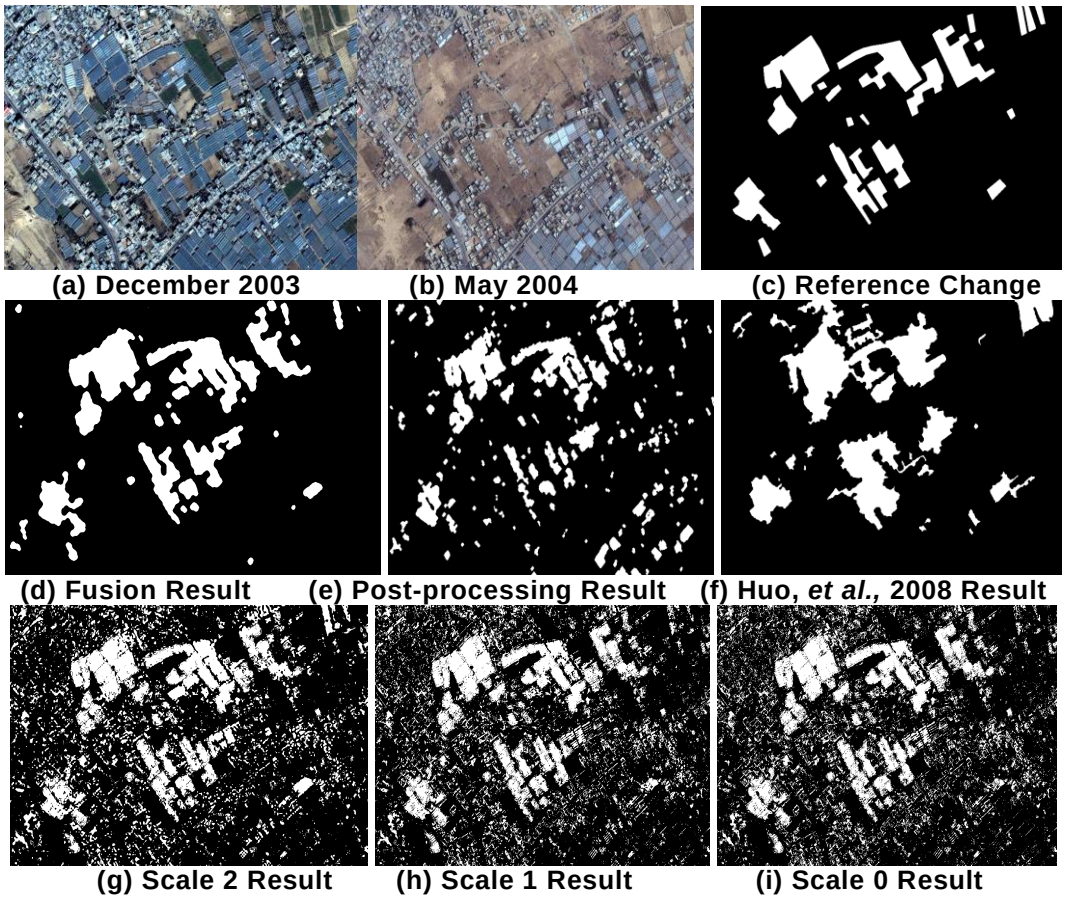

Figure 2. Test Data and Processed Result Comparison

The other example is shown in Figure 3. It is an airport image including a number of aircrafts (Figure 3(a)); in the changed image (Figure 3(b)), six aircrafts are disappeared (see Figure 3(a) arrows); the processing results are shown in Figure 3(c-d). The aircrafts are detected clearly by using the algorithm.

Table 1. Property Comparison of the Change Detection Result Through Different Methods

Result from	Detection rate	Accuracy	Kappa coefficient
The paper result	87.40%	76.89%	79.07%
The post-processing result	68.75%	60.88%	59.26%
The scale 2 result	80.59%	44.46%	49.26%
The scale 1 result	78.83%	43.00%	47.25%
The scale 0 result	77.81%	41.94%	45.84%
The literature 4 result	58.76%	44.90%	42.95%

Copyright ⓒ 2015 SERSC

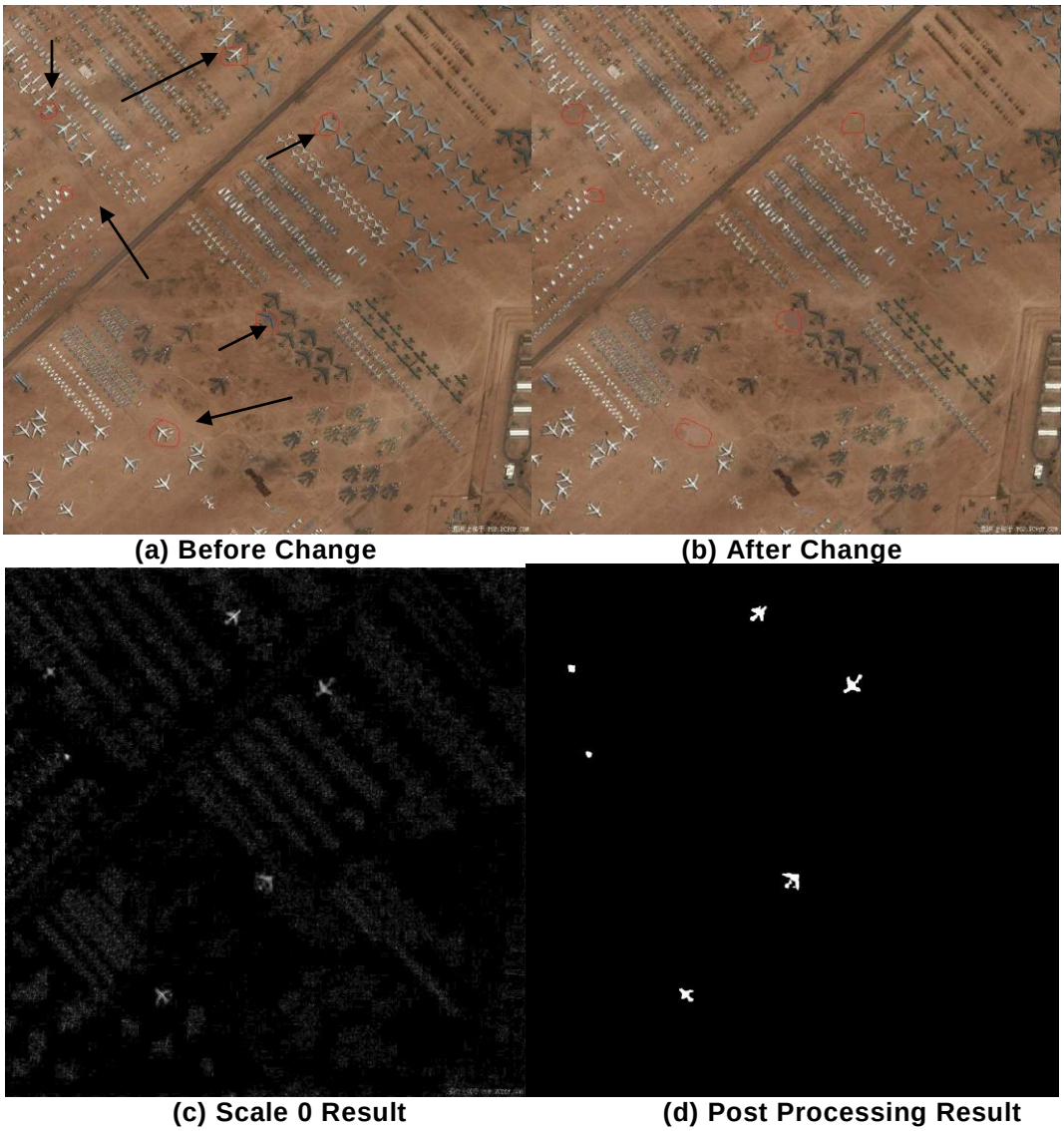

(a) Before Change (b) After Change

(c) Scale 0 Result (d) Post Processing Result

Figure 3. Test Data and Processed Result at an Airport

From the test result, the several conclusions are:

(a) The change detection results at different scales are different.

(b) The change detection result at a low scale is easily to be affected by the registration error, so its accuracy is low and the more noise occur.

(c) The change detection result image at a high scale includes less noise, but at the same time it enhances a leak alarm rate. However one can detect the change information at a high scale, which is not detected at a low scale, such as that the green land change is detected more accurately at a higher scale, so the detection rate and accuracy at a high scale are improved.

(d) About the post-processing for the change detection result, its accuracy is improved because of the registration error suppression, and the detection rate decreases due to the wrong detection result at the same time, but in total, the detection effect is better than that at each single scale.

(e) The change detection result by using the new algorithm is improved significantly comparing with the others, its main reason is that the Markov random field fusion algorithm takes full account of the correlation between the adjacent pixels and the links of the different scale change detection results, and

Copyright ⓒ 2015 SERSC

it is also because of effectively inhabit noise by registration error at each single scale.

(f) In this study, a watershed segmentation algorithm is used to extract objects, and then the change detection result is obtained based on the object level decision class fusion [4], and the result image is in Figure 2(f). From the test result image and Table 1, the detection rate and accuracy in the above algorithm are low, because the object, in which only a part of the object is changed, cannot be decided correctly. The studied new algorithm belongs to pixel level fusion and the algorithm (Huo, *et al.,* 2008) [7] belongs to object level fusion. Both of them are robust to the registration error and the angle error, but the new algorithm is not affected by the object extraction accuracy and the literature [7] algorithm has certain singularity to the object in which only a part is changed.

6. Conclusions

The paper presents a change detection algorithm which uses the wavelet transform and the Markov random field fusion to process change detection results at different scales, and takes full account of the correlation between the adjacent pixels and the links of the change detection results at different scales. The fusion results are more accurate and practical. The Mahalanobis distance is applied to the change detection for different scale images. The Mahalanobis distance decision function is a hyper-ellipsoidal decision surface in a high dimensional feature space; therefore, it is more effective to decide the change and the non-change pixels/areas than other algorithms. The test and analysis prove that the change detection results at different scales are influential to the final Markov random field fusion result. And the Markov random field is not only suitable to the fusion of the multi-scale change detection results, but also the fusion of the change detection results through the other algorithms. Since the algorithm is newly studied both in theory and practice, the experimental results and the algorithm comparison are limited, hence, in this case, the studied algorithm needs to be further improved, In addition, the threshold value for the Mahalanobis distance decision should be decided by a theoretical algorithm based on some new theory in the previous study [20], and a number of post processing functions should be improved based on other new image segmentation algorithms [21-22].

Acknowledgements

This research is financially supported by Shaanxi special funds for major scientific and technological innovation projects (No. 2007ZKC (-) 02-01), the Science and Technology Bureau of Shaanxi Province in China with number 2013KW03, and Special Fund for Basic Scientific Research of Central Colleges, Chang'an University in China (grant no. CHD2013G2241019) in China.

References

[1] S. Jin, L. Yang and P. Danielson, "A comprehensive change detection method for updating the national land cover database to circa 2011", Remote Sensing of Environment, vol. 132, **(2013)**, pp. 159-175.
[2] M. Forkel, N. Carvalhais, J. Verbesselt, M. D. Mahecha, S. R. N. Christopher and M. Reichstein, 'Trend Change Detection in NDVI Time Series: Effects of Inter-Annual Variability and Methodology", Remote Sens., vol. 5, no. 5, **(2013),** pp. 2113-2144, doi:10.3390/rs5052113.
[3] Z. Zhu and E. W. Curtis, "Continuous change detection and classification of land cover using all available Landsat data", Remote Sensing of Environment, vol. 144, no. 25, **(2014)**, pp. 152–171.
[4] R. J. Radke, S. Andra, O. AI-Kofahi and B. Roysam, "Image change detection algorithms: a systematic survey", IEEE Trans on Image Processing, vol. 14, no.3, **(2005)**, pp. 294-307.

 Copyright ⓒ 2015 SERSC

[5] J. Gong, H. Sui, G. Ma and Q. Zhou, "A review of multi-temporal remote sensing data change detection algorithms. The International Archives of the Photogrammetry", Remote Sensing and Spatial Information Sciences, vol. 37, no. B7, **(2008)**, pp. 757-762.
[6] X. Dai X. And K. Siamak, "The Effects of Image Misregistration on the Accuracy of Remotely Sensed Change Detection", IEEE Trans on Geoscience and Remote Sensing, vol. 36, no. 5, **(1998)**, pp. 1566-1577.
[7] Ch. L. Huo, J. Cheng, H. Q. Lu and Z. X. Zhou, "Object-level Change Detection Based on Multiscale Fusion. Acta Automatic Sinica", vol. 34, no. 3, **(2008)**, pp. 251-257.
[8] G. H. Geoffrey, "Object-level change detection in spectral imagery. IEEE Trans on Geoscience and Remote Sensing", vol. 39, no. 3, **(2001)**, pp. 553-561.
[9] G. Chen, J. H. Geoffrey, L. M. T. Carvalho and M. A. Wulder , "Object-based change detection", International Journal of Remote Sensing, vol. 33, no. 14, **(2012)**, pp. 4434–4457.
[10] J. Su, X. Lin and D. Liu, "Change detection algorithm for remote sensing images based on object matching", Journal of Tsinghua University (Natural Science Edition), vol. 47, no. 10, **(2007)**, pp. 1610-1613.
[11] C. Turgay, "Multiscale Change Detection in Multitemporal Satellite Images", IEEE Geoscience and Remote Sensing Letters, vol. 6, no. 4, **(2009)**, pp. 1-5.
[12] B. Francesca and B. Lorenzo, "A Detail-Preserving Scale-Driven Approach to Change Detection in Multitemporal SAR Images", IEEE Trans on Geoscience and Remote Sensing, vol. 43, no. 12, **(2005)**, pp. 2963-2972.
[13] K. Arai, "Wavelet Based Change Detection for Four Dimensional Assimilation Data in Space and Time Domains", (IJACSA) International Journal of Advanced Computer Science and Applications, vol. 3, no. 11, **(2012)**, pp. 71-75.
[14] Y. Chen and Z. G. Cao, "Change detection of multispectral remote-sensing images using stationary wavelet transforms and integrated active contours", International Journal of Remote Sensing, vol. 34, no. 24, **(2013)**, pp. 8817-8837.
[15] M. Farid and B. Yakoub, "Markovian Fusion Approach to Robust Unsupervised Change Detection in Remotely Sensed Imagery", IEEE Geoscience and Remote Sensing Letters, vol. 3, no. 4, **(2006)**, pp. 457-461.
[16] C. H. Wang, N. K. Komodakis and N. K. Paragios, "Markov Random Field modeling, inference & learning in computer vision & image understanding: A survey", Computer Vision and Image Understanding, vol. 117, no. 11, **(2013)**, pp. 1610–1627.
[17] Z. Stan and J. Li, Editor, Markov Random Field Modeling in Image Analysis. Springer Berlin publisher, **(2001)**.
[18] A. Ghosh, N. B. Subudhi and L. Bruzzone, "Integration of Gibbs Markov random field and Hopfield-type neural networks for unsupervised change detection in remotely sensed multitemporal images", IEEE Trans Image Process, vol. 22, no. 8, **(2013)**, pp. 3087-3096, doi: 10.1109/TIP.2013.2259833.
[19] S. Z. Li, Markov Random Field Modeling in Image Analysis, New York: NY, USA: Springer-Verlag **(2001)**.
[20] W. X. Wang, W S Li and X Yu, "Fractional differential algorithms for rock fracture images", The Imaging Science Journal, vol. 60, **(2012)**, pp. 103-111.
[21] W. X. Wang, "Colony image acquisition system and segmentation algorithms", Optical Engineering, vol. 50, no. 12, **(2011)**, pp. 123001.
[22] W. X. Wang, X. Zhang, T. Cao, L. P. Tian, S. Liu and Z. W. Wang, "Fuzzy and Touching Cell Extraction on Modified Graph MST and Skeleton Distance Mapping Histogram", Journal of Medical Imaging and Health Informatics, vol. 4, no. 3, **(2014)**, pp. (2156-7018/2014/4) 001-008, doi:10.1166/jmihi.2014.1264.

Authors

Song Hongxun, Associate professor in Chang'an University, China. In 1982, he obtained Bachelor degree in Changchun University of Science and Technology, China, and in 1986, he obtained Master degree in Xi'an institute of optics and precision mechanics of CAS, China. His interests include road traffic photoelectric detection technology, laser displacement sensors and photoelectric detection system, and image processing.

Copyright ⓒ 2015 SERSC

Wang Weixing, Professor in Information engineering. He obtained his PhD degree in 1997 at Royal Institute of Technology in Sweden, since 2001, he has been a PhD supervisor at Royal Institute of Technology, now he is a visiting professor at Chang'an University, and his interests involve Information engineering, Image processing and analysis, Pattern recognition and Computer Vision.

Zhang Tingting, Master student in Information Engineering. In 2014, she obtained her Bachelor degree in Chang'an University, China. Now she is in graduate school, her major is Computer application technology. Her interests include Information engineering; Level set method, Image processing and Matlab software.

Copyright ⓒ 2015 SERSC